TRANSACTIONS ON ELECTRICAL AND ELECTRONIC MATERIALS
Vol. 11, No. 3, pp. 112-115, June 25, 2010

Invited Paper

pISSN: 1229-7607 eISSN: 2092-7592
DOI: 10.4313/TEEM.2010.11.3.112

Characterizations of Highly Ordered TiO_2 Nanotube Arrays Obtained by Anodic Oxidation

Hun Park and Ho-Gi Kim†
Department of Materials Science and Engineering, Korea Advanced Institute of Science and Technology, Daejeon 305-701, Korea

Won-Youl Choi†
Department of Metal and Materials Engineering, Kangnung-wonju National University, Kangnung 210-702, Korea

Received May 4, 2010; Accepted May 13, 2010

This paper provides the properties of TiO_2 nanotube arrays which are fabricated by anodic oxidation of Ti metal. Highly ordered TiO_2 nanotube arrays could be obtained by anodic oxidation of Ti foil in 0.3 wt·% NH_4F contained ethylene glycol solution at 30°C. The length, pore size, wall thickness, tube diameter etc. of TiO_2 nanotube arrays were analyzed by field emission scanning electron microscopy. Their crystal properties were studied by field emission transmission electron microscopy and X-ray photoelectron spectroscopy.

Keywords: TiO_2, Nanotube, Anodic oxidation, Ordered structure

1. INTRODUCTION

One-dimensional porous TiO_2 nanotube structures have received great attentions for applications in photovoltaics [1-5], gas sensors [6], electrochromic devices [7], Li-secondary batteries [8], etc. TiO_2 nanotubes have been fabricated by various methods such as deposition into a nanoporous alumina template [9], sol-gel transcription using organo-gelators as templates [10], seeded growth [11], hydrothermal processes [12], and anodization processes [13,14]. Highly ordered TiO_2 nanotube arrays, which have by far the most remarkable properties, can be made by anodic oxidation of titanium in fluoride-based baths [15].

Electrolyte composition and its pH determine both the rate of nanotube formation and the rate at which the resultant oxide is dissolved. Several aqueous electrolytes such as HF/H_2O [13], H_2SO_4/H_2O [16], $HF\text{-}CrO_4/H_2O$ [17], and $KF/NaF/H_2O$ [18] have recently been used to create TiO_2 nanotube arrays. However, there is a limitation to increase the thickness of TiO_2 nanotube arrays in aqueous electrolyte solution due to the vigorous chemical dissolution of the oxide by fluorine ions [15]. With organic electrolytes, the donation of oxygen is more difficult compared to water, thus reducing the tendency to form oxide. At the same time, the reduction in water content reduces the chemical dissolution of the oxide in the fluorine containing electrolytes and hence aids the longer-nanotube formation [15]. These organic electrolytes include dimethyl sulfoxide, formamide, ethylene glycol, and N-methylformamide [19]. Paulose et al. [20] fabricated mechanically stable TiO_2 nanotube arrays up to 1,000 μm in length by using ethylene glycol electrolyte containing 0.6 wt·% NH_4F and 3.5 vol·% H_2O.

In this study, we prepared TiO_2 nanotube arrays by anodic oxidation of Ti metal in ethylene glycol solution. Several properties of TiO_2 nanotube arrays such as crystal structure, morphology, current-time behavior during anodization, etc., were studied.

2. EXPERIMENTS

Highly ordered TiO_2 nanotube arrays were fabricated by anodic oxidation of 0.5 mm thick Ti foil (99.0%, Alfar Aesar, Word Hill, Massachusetts, USA) at a constant potential 60 V (ramping up to 60 V with a ramping speed 1 V/s) in the ethylene glycol solution containing 0.3 wt·% NH_4F and 2 vol·% H_2O. The anodized samples were annealed at 500°C for 60 minutes to crystallize the amor-

† Author to whom all correspondence should be addressed:
E-mails: hgkim@kaist.ac.kr, cwy@kangnung.ac.kr

phous TiO_2 nanotube arrays. Pt metal was used as a counter electrode. The anodization voltage was applied by a DC power supply (Model XKW600-1.7, Xantrex Technology, Inc., Burnaby, Canada). Current-transient curve was measured during anodization using a digital multimeter (Model 34401A, Agilent Technologies, Inc., Santa Clara, CA, USA) interfaced with a computer. Power supply and multimeter were computer-controlled with GPIB interface and LabVIEW program (National Instrument, Austin, TX, USA).

The length, pore size, diameter, and wall thickness of TiO_2 nanotube arrays were determined by field emission scanning electron microscopy (FESEM, Philips XL 30SFEG; Philips, Amsterdam, Netherlands) analysis. Crystal properties of TiO_2 nanotube arrays were studied by X-ray diffractometry (XRD, Rigaku D/MAX-RC, Cu*K*α radiation; Rigaku, Tokyo, Japan) and field emission transmission electron microscopy (FETEM, Tecnai G^2 F30 S-TWIN; FEI, Hilsboro, OR, USA) analysis. X-ray photoelectron spectroscopy (XPS, Thermo VG Scientific ESCA 2000; Thermo Fisher Scientific, Waltham, MA, USA) analysis was introduced to study the chemical composition and the bonding energy of Ti and O ions in crystallized TiO_2 nanotube arrays.

3. RESULTS AND DISCUSSION

Figure 1 shows current-transient curves obtained during anodic oxidation of Ti foil. Figure 1(a) gives the current-time behavior when the anodization voltage increases from 0 V to 60 V at the ramping speed of 1 V/s. In the early stage of voltage ramping, the current, which flows from Ti anode to Pt cathode, abruptly decreases due to the formation of thin TiO_2 layer on Ti foil. However, after ~4 seconds, the current increases in proportion to the ramping time. It seems that the as-formed TiO_2 layer on Ti foil is not thick enough to block the current flow thus the current is proportional to the ramping voltage.

A current-transient curve obtained at a constant voltage of 60 V during anodizing process can be shown in Fig. 1(b). At the beginning the current increases to some extent because etching of thin TiO_2 layer on Ti foil by F ions exposes Ti metal. However, the exposed surface of Ti metal is readily converted to thin TiO_2 layer thus the current decreases according to the anodizing time. TiO_2 nanotube structures start to be formed from the moment at which the current decreases. Directional etching of TiO_2 and Ti by F^- ions induced by an applied voltage makes possible to fabricate highly ordered TiO_2 nanotube arrays.

Figure 2 shows FESEM images of TiO_2 nanotube arrays obtained by anodic oxidation of Ti foil in 0.3 wt·% NH_4F contained ethylene glycol solution. Figures 2(a)-(c) give the cross-section images obtained by anodization at a constant voltage of 60 V for 20, 30, and 40 minutes, respectively. The thickness of TiO_2 nanotube arrays increased from 18 μm for 20 minutes anodization to 30.8 μm for 40 minutes anodization. In ethylene glycol solution, the movement of F^- ions is slow thus the etching speed for the surface of TiO_2 nanotube arrays is lower than that in aqueous solution [15, 19, 20]. Longer nanotube arrays up to 1,000 μm can be obtained by controlling NH_4F concentration, anodizing time, anodizing voltage, etc. [20]. The bottom and cross-section images of TiO_2 nanotube arrays can be shown in Fig. 2(d). TiO_2 nanotube arrays were close-packed together and the bottom of each TiO_2 nanotube was blocked. The diameter, wall thickness, pore size of each TiO_2 nanotube were ~120 nm, ~40 nm, ~40 nm, respectively.

Figure 3 shows FETEM images of annealed TiO_2 nanotube arrays. Figure 3(a) is the magnified image of part A in the inset figure and Fig. 3(b) gives the magnified image of part B in Fig. 3(a). There are several crystal fringes in Fig. 3(a) and each fringe has a different orientation. From these results, we can know that the annealed TiO_2 nanotube arrays have a polycrystalline structure

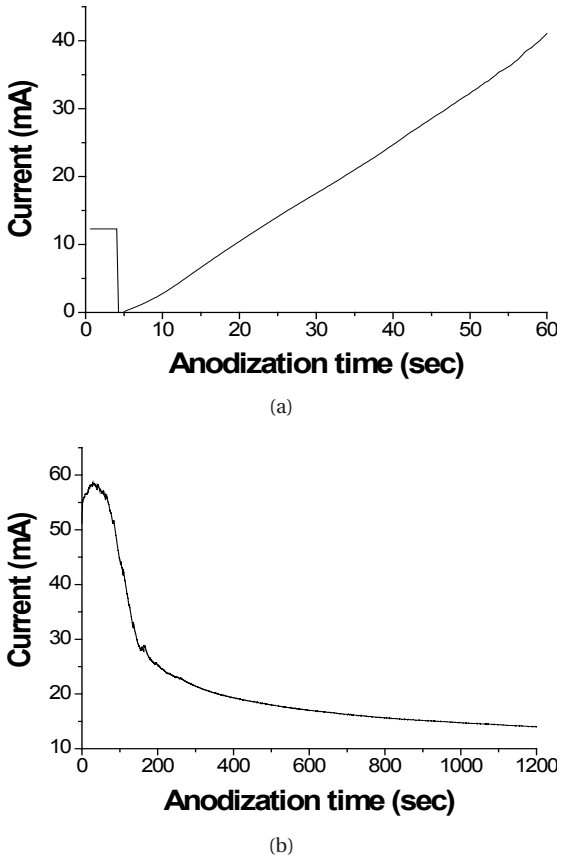

Fig. 1. Current-transient curve during anodization of Ti foil; (a) when ramping a voltage from 0 V to 60 V (b) at a constant voltage of 60 V.

which is composed of several crystal grains. It seems that each fringe represents a TiO_2 single-crystal grain. Ordered arrays of Ti and O atoms in annealed TiO_2 nanotube arrays are shown in Fig. 3(b). The high resolution TEM image (Fig. 3(b)) shows $(0\bar{1}1)$, $(0\bar{2}0)$, and (002) atomic planes with a diffraction direction of z axis [100] zone. The interfacial angle of $(0\bar{1}1)$ and (002) is 68.3° and that of $(0\bar{2}0)$ and (002) is 90°. Lattice spaces of $(0\bar{1}1)$ and (002) are 3.51 Å and 4.76 Å, respectively. These values of interfacial angles and lattice spaces are identical to theoretical values of anatase TiO_2 crystal structure [21].

The as-anodized TiO_2 nantoube arrays have an amorphous structure (data not shown here). After heat treatment at 500°C for 1 hour, the amorphous TiO_2 nanotube arrays are converted to anatase polycrytalline structure. It can be shown from the results of FETEM analysis that anatase phase of TiO_2 nanotube arrays could be successfully formed by heat treatment.

Figure 4 shows XPS results of annealed TiO_2 nanotube arrays. Three characteristic peaks of Ti and O can be observed in Figs. 4(a) and (b). The binding energies of Ti $2p_{1/2}$, Ti $2p_{3/2}$, and O 1s peaks are 465.3 eV, 459.4 eV, and 530.6 eV, respectively. The difference of binding energies of Ti $2p_{1/2}$ and Ti $2p_{3/2}$ can be seen as 5.9 eV in Fig. 4(a). This means that Ti has a tetravalent state in TiO_2 nanotube arrays [22]. The measured binding energies of 465.3 eV for the Ti $2p_{1/2}$ peak, 459.4 eV for the Ti $2p_{3/2}$ peak, and 530.6 eV for the O 1s peak are in excellent agreement with the previously published results of anatase TiO_2 crystal structure [22,23].

4. CONCLUSIONS

Highly ordered TiO_2 nanotube arrays were fabricated by using

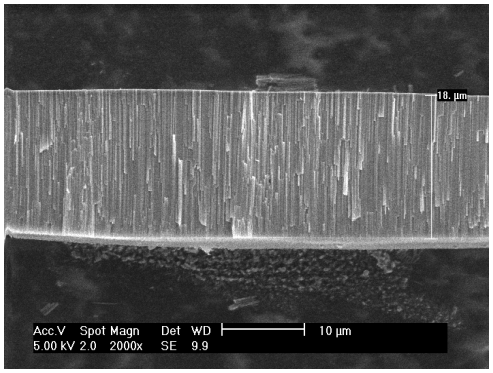

(a)

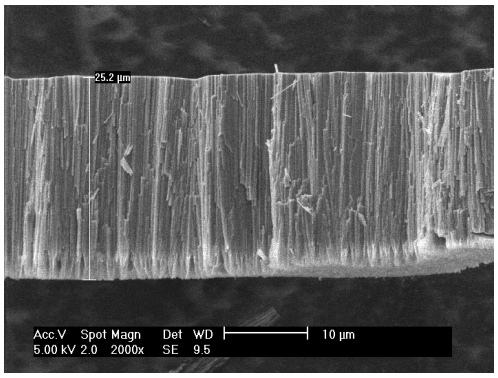

(b)

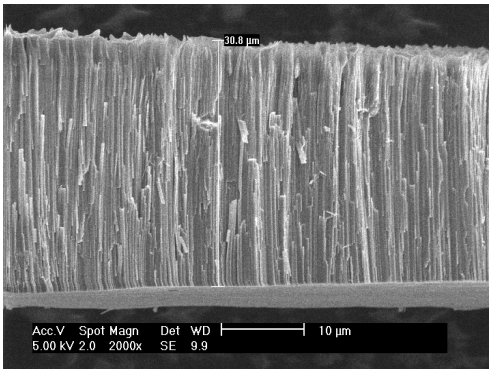

(c)

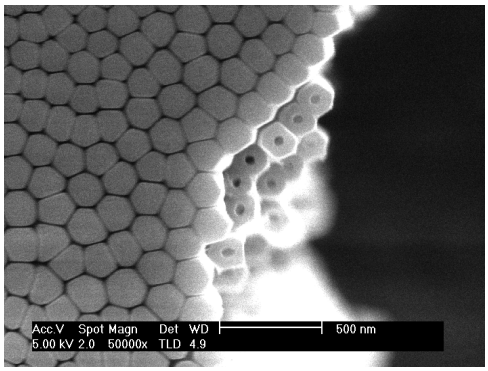

(d)

Fig. 2. Field emission scanning electron microscopy images of TiO_2 nanotube arrays which was fabricated by anodic oxidation of Ti metal; (a) samples anodized for 20 minutes (b) samples anodized for 30 minutes (c) samples anodized for 40 minutes (d) bottom and cross-section images of TiO_2 nanotube arrays.

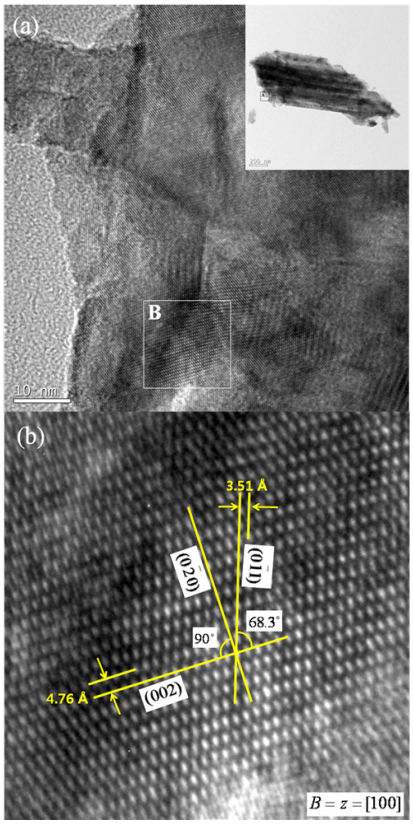

Fig. 3. Field emission transmission electron microscopy images of annealed TiO_2 nanotube arrays; (a) magnified image of A in the inset figure, (b) magnified image of B in Fig. 3(a).

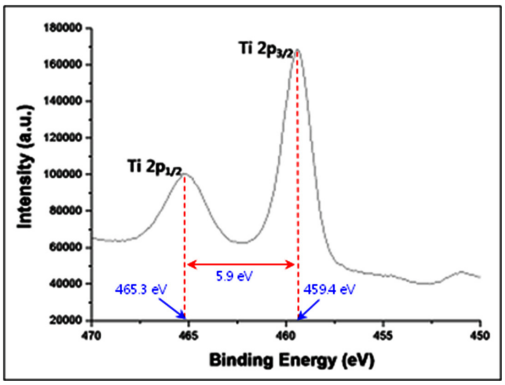

(a)

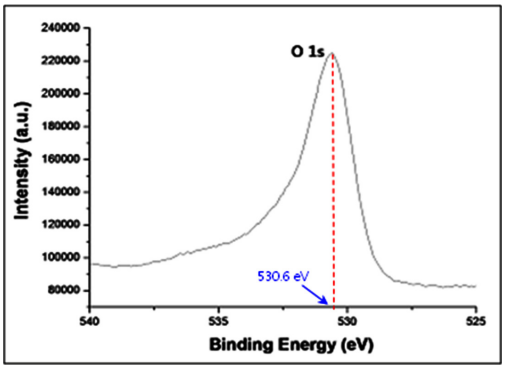

(b)

Fig. 4. X-ray photoelectron spectroscopy results of annealed TiO_2 nanotube arrays; (a) Ti 2p peaks (b) O 1s peak.

anodization process. As-anodized TiO_2 nanotube arrays had an amorphous structure. After heat treatment of as-anodized samples, anatase phase of TiO_2 nanotube arrays could be obtained. FESEM analysis showed the successful formation of highly ordered TiO_2 nanotube arrays by anodic oxidation of Ti foil. We could confirm the conversion of crystal phase of TiO_2 nanotube arrays from amorphous to anatase crystalline by FETEM and XPS.

ACKNOWLEDGMENTS

This work was financially supported by Basic Science Research Program through the National Research Foundation of Korea (NRF) funded by the Ministry of Education, Science and Technology (2009-0075181).

REFERENCES

[1] G. K. Mor, K. Shankar, M. Paulose, O. K. Varghese, and C. A. Grimes, Nano Lett. **6**, 215 (2006) [DOI: 10.1021/nl052099j].
[2] H. Park, D. J. Yang, J. S. Yoo, K. S. Mun, W. R. Kim, H. G. Kim, and W. Y. Choi, J. Ceram. Soc. Jpn. **117**, 596 (2009) [DOI: 10.2109/jcersj2.117.596].
[3] H. Park, D. J. Yang, H. G. Kim, S. J. Cho, S. C. Yang, H. Lee, and W. Y. Choi, J. Electroceram. **23**, 146 (2009) [DOI: 10.1007/s10832-007-9341-x].
[4] D.J. Yang, H. Park, S. J. Cho, H. G. Kim, and W. Y. Choi, J. Phys. Chem. Solids **69**, 1272 (2008) [DOI: 10.1016/j.jpcs.2007.10.107].
[5] H. Park, W. R. Kim, H. T. Jeong, J. J. Lee, H. G. Kim, and W. Y. Choi, Sol. Energy Mater. Sol. Cells in press [DOI: 10.1016/j.solmat.2010.02.017].
[6] G. K. Mor, M. A. Carvalho, O. K. Varghese, M. V. Pishko, and C. A. Grimes, J. Mater. Res. **19**, 628 (2004) [DOI: 10.1557/JMR.2004.0079].
[7] A. Ghicov, H. Tsuchiya, R. Hahn, J. M. Macak, A. G. Munoz, and P. Schmuki, Electrochem. Comm. **8**, 528 (2006) [DOI: 10.1016/j.elecom.2006.01.015].
[8] G. F. Ortiz, I. Hanzu, T. Djenizian, P. Lavela, J. L. Tirado, and P. Knauth, Chem. Mater. **21**, 63 (2009) [DOI: 10.1021/cm801670u].
[9] P. Hoyer, Langmuir **12**, 1411 (1996) [DOI: 10.1021/la9507803].
[10] J. H. Jung, H. Kobayashi, K. J. C. van Bommel, S. Shinkai, and T. Shimizu, Chem. Mater. **14**, 1445 (2002) [DOI: 10.1021/cm011625e].
[11] Z. R. Tian, J. A. Voigt, J. Liu, B. McKenzie, and H. Xu, J. Am. Chem. Soc. **125**, 12384 (2003) [DOI: 10.1021/ja0369461].
[12] T. Kasuga, M. Hiramatsu, A. Hoson, T. Sekino, and K. Niihara, Langmuir **14**, 3160 (1998) [DOI: 10.1021/la9713816].
[13] D. Gong, C. A. Grimes, O. K. Varghese, W. Hu, R. S. Singh, Z. Chen, and E. C. Dickey, J. Mater. Res. **16**, 3331 (2001) [DOI: 10.1557/JMR.2001.0457].
[14] J. M. Macak, H. Tsuchiya, and P. Schmuki, Angew. Chem. Int. Ed. **44**, 2100 (2005) [DOI: 10.1002/anie.200462459].
[15] G. K. Mor, O. K. Varghese, M. Paulose, K. Shankar, and C. A. Grimes, Sol. Energy Mater. Sol. Cells **90**, 2011 (2006) [DOI: 10.1016/j.solmat.2006.04.007].
[16] R. Beranek, H. Hildebrand, and P. Schmuki, Electrochem. Solid-State Lett. **6**, B12 (2003) [DOI: 10.1149/1.1545192].
[17] V. Zwilling, E. Darque-Ceretti, A. Boutry-Forveille, D. David, M. Y. Perrin, and M. Aucouturier, Surf. Interface Anal. **27**, 629 (1999) [DOI: 10.1002/(SICI)1096-9918(199907)27:7<629::AID-SIA551>3.0.CO;2-0].
[18] Q. Y. Cai, M. Paulose, O. K. Varghese, and C. A. Grimes, J. Mater. Res. **20**, 230 (2005) [DOI: 10.1557/JMR.2005.0020].
[19] M. Paulose, K. Shankar, S. Yoriya, H. E. Prakasam, O. K. Varghese, G. K. Mor, T. A. Latempa, A. Fitzgerald, and C. A. Grimes, J. Phys. Chem. B **110**, 16179 (2006) [DOI: 10.1021/jp064020k].
[20] M. Paulose, H. E. Prakasam, O. K. Varghese, L. Peng, K. C. Popat, G. K. Mor, T. A. Desai, and C. A. Grimes, J. Phys. Chem. C **111**, 14992 (2007) [DOI: 10.1021/jp075258r].
[21] U. Diebold, Surf. Sci. Rep. **48**, 53 (2003) [DOI: 10.1016/S0167-5729(02)00100-0].
[22] J. H. Kim, S. Lee, and H. S. Im, Appl. Surf. Sci. **151**, 6 (1999) [DOI: 10.1016/S0169-4332(99)00269-X].
[23] Y. Choi, T. Umebayashi, and M. Yoshikawa, J. Mater. Sci. **39**, 1837 (2004) [DOI: 10.1023/B:JMSC.0000016198.73153.31].